A Novel Numerical Approach for the Analysis of 2D MEMS-Based Variable Capacitors Including the Effect of Arbitrary Motions

Michiko Kuroda **Noriyuki Miura**

kuroda@cc.teu.ac.jp

School of Engineering, Tokyo University of Technology, Hachioji, Tokyo 192-0982, Japan

Manos M. Tentzeris

School of ECE, Georgia Institute of Technology, Atlanta, GA 30332-250, USA

Abstract

A novel time-domain technique is proposed for the analysis of MEMS-based variable devices involving motion to arbitrary in-plane directions using the adaptive body fitted grid generation method with moving boundaries. MEMS technology is growing rapidly in the RF field and the accurate design of RF MEMS switches that can be used for phase shifting or reconfigurable tuners requires the computationally effective modeling of their transient and steady-state behavior including the accurate analysis of their time-dependent moving boundaries. Due to the limitations of the conventional time-domain numerical techniques, it is tedious to simulate these problems numerically. The new technique proposed in this paper is based on the time-difference time-domain method with an adaptive implementation of grid generation. Employing this transformation, it is possible to apply the grid generation technique to the analysis of geometries with time-changing boundary conditions. A variable capacitor that consists of two metal plates that can move to arbitrary in-plane directions is analyzed as a benchmark. The numerical results expressing the relationship between the velocity of the plates and the capacitance are shown and the transient effect is accurately modeled.

1. Introduction

The accurate knowledge of the electromagnetic field variation for a moving or rotating body is very important for the realization of new optical or microwave devices, such as the RF-MEMS structures used in phase-shifters, couplers or filters [1,2]. Computational method for moving boundary problems have been presented earlier in heat and fluid flow area [3-6]. In this paper, we propose a new numerical approach for the analysis of this type of problems that alleviates the limitations of the conventional time-domain techniques in the electromagnetic field [7-12] and shows good agreement with analytical results [13]. Employing the transformation with the time factor, it is possible to apply the grid generation technique of [14] to the time-domain analysis of geometries with moving objects. With such a grid, the FD-TD method can be solved very easily on a “static” (time-invariant) rectangular mesh regardless of the shape and the motion of the physical region, something that makes it an especially good tool to analyze arbitrary shape and motion. In this paper, this simulation method is applied to the analysis of a two-dimensional MEMS variable capacitor with arbitrary in-plane motions of its interdigitated fingers.

2. General Theory of the Body-Fitted Grid Generation Method with Moving Boundaries

This technique is based on the finite-difference time-domain (FD-TD) method with an adaptive implementation of grid generation. The key feature of this method is that the time factor is added to the conventional numerical grid generation. We have improved the grid generation of [14] to the present one having a coordinate line coincident with arbitrarily shaped moving boundaries or moving bodies. Employing this transformation, it is possible to apply the grid generation technique to the analysis of geometries with time-changing boundary conditions. With such a grid, the FD-TD method can be solved very easily using a time-invariant square grid (rectangular computational region) regardless of the shape and the motion of the physical region. Employing the transformation with the time factor, the partial differential equation in the physical region (x, y, z, t) is related to the computational region $(\xi, \eta, \varsigma, \tau)$ as follows

$$x = x(\xi, \eta, \varsigma, \tau), \tag{1}$$

$$y = y(\xi, \eta, \varsigma, \tau), \tag{2}$$

$$z = z(\xi, \eta, \varsigma, \tau), \tag{3}$$

$$t = t(\xi, \eta, \varsigma, \tau). \tag{4}$$

The inverse transformation is given by

$$\xi = \xi(x, y, z), \tag{5}$$

$$\eta = \eta(x, y, z), \tag{6}$$

$$\varsigma = \varsigma(x, y, z), \tag{7}$$

$$\tau = \tau(x, y, z). \tag{8}$$

According to the transformation, the first derivatives are transformed as follows,

$$\begin{bmatrix} \partial/\partial x \\ \partial/\partial y \\ \partial/\partial z \\ \partial/\partial t \end{bmatrix} = K \begin{bmatrix} \partial/\partial \xi \\ \partial/\partial \eta \\ \partial/\partial \varsigma \\ \partial/\partial \tau \end{bmatrix} \tag{9}$$

The inverse transformation is given by,

$$\begin{bmatrix} \partial/\partial \xi \\ \partial/\partial \eta \\ \partial/\partial \varsigma \\ \partial/\partial \tau \end{bmatrix} = L \begin{bmatrix} \partial/\partial x \\ \partial/\partial y \\ \partial/\partial z \\ \partial/\partial t \end{bmatrix} \tag{10}$$

where the matrices *K* and *L* are given by

$$K = \begin{bmatrix} \partial\xi/\partial x & \partial\eta/\partial x & \partial\varsigma/\partial x & \partial\tau/\partial x \\ \partial\xi/\partial y & \partial\eta/\partial y & \partial\varsigma/\partial y & \partial\tau/\partial y \\ \partial\xi/\partial z & \partial\eta/\partial z & \partial\varsigma/\partial z & \partial\tau/\partial z \\ \partial\xi/\partial t & \partial\eta/\partial t & \partial\varsigma/\partial t & \partial\tau/\partial t \end{bmatrix} \tag{11}$$

and

$$L = K^{-1} = \begin{bmatrix} \partial x/\partial \xi & \partial y/\partial \xi & \partial z/\partial \xi & \partial t/\partial \xi \\ \partial x/\partial \eta & \partial y/\partial \eta & \partial z/\partial \eta & \partial t/\partial \eta \\ \partial x/\partial \varsigma & \partial y/\partial \varsigma & \partial z/\partial \varsigma & \partial t/\partial \varsigma \\ \partial x/\partial \tau & \partial y/\partial \tau & \partial z/\partial \tau & \partial t/\partial \tau \end{bmatrix}. \tag{12}$$

By this transformation, there is a unique correspondence between the computational region and the physical region. The transformed region can be easily solved in the rectangular computational region by FD-TD method. The stability criterion for FD-TD algorithm is discussed in [8].

3. Two Dimensional Variable Capacitor with Arbitrary Motions

The geometry to be considered here is shown in Fig. 1. Under the combined effect of mechanical and electrical force, the two plates are assumed to move with different velocities to arbitrary in-plane directions. For the two-dimensional TM-propagation case, there are only Ex, Ey, Hz nonzero components with a time variation given by the following equations,

$$\frac{\partial H_z}{\partial t} = \frac{1}{\mu}\left(\frac{\partial E_x}{\partial y} - \frac{\partial E_y}{\partial x}\right), \tag{13}$$

$$\frac{\partial E_x}{\partial t} = \frac{1}{\varepsilon}\left(\frac{\partial H_z}{\partial y} - J_x\right), \tag{14}$$

$$\frac{\partial E_y}{\partial t} = -\frac{1}{\varepsilon}\left(\frac{\partial H_z}{\partial x} + J_y\right), \tag{15}$$

where ε, μ are the constitutive parameters of the respective media. In Fig. 1, the configurations of the physical and of the computational regions are shown. The interdigitated fingers are assumed to move to arbitrary directions in the *xy*-plane with velocities v and u, respectively and the direction of their motion is shown by the angles θ_v and θ_u. Using a coordinates' transformation technique, the time-changing physical region (*x*,*y*,*t*) can evolve to a time-invariant computational domain (ξ, η, τ). To transform the equations, it is easy to separate the physical region in 25 subregions, where (n, m) are the indices of each subregion in *x*- and *y*-direction. The number of subregions depends on the geometry of the moving parts of the geometry.

Different subregions are characterized by different velocities in amplitude and/or direction. The transform equations between the physical and the computational regions are chosen as

$$\xi = \alpha_{n-1} \frac{x - h_{n-1}(t)}{h_n(t) - h_{n-1}(t)} + \xi_{n-1}, \tag{16}$$

$$\eta = \beta_{m-1} \frac{y - g_{m-1}(t)}{g_m(t) - g_{m-1}(t)} + \eta_{m-1}, \tag{17}$$

$$\tau = t \tag{18}$$

where n=1, 2, 3, 4, 5 m=1, 2, 3, 4, 5 and $h_0(t)$, $h_1(t)$, $h_2(t)$, $h_3(t)$, $h_4(t)$, $h_5(t)$, $g_0(t)$, $g_1(t)$, $g_2(t)$, $g_3(t)$, $g_4(t)$, $g_5(t)$ are written in the following form assuming that the plate velocities remain constant for the whole time of their motion. α_{n-1} , β_{m-1} are coefficients to normalize the computational region. The coordinates x_1, x_2, x_3, x_4 , and y_1, y_2, y_3, y_4 represent the initial positions of the plates,

$$h_1(t) = x_1 + (v \cos\theta_v)t\ , \tag{19}$$

$$h_2(t) = x_2 + (u \cos\theta_u)t\ , \tag{20}$$

$$h_3(t) = x_3 + (v \cos\theta_v)t\ , \tag{21}$$

$$h_4(t) = x_4 + (u \cos\theta_u)t\ , \tag{22}$$

$$g_1(t) = y_1 + (u \sin\theta_u)\ t\ , \tag{23}$$

$$g_2(t) = y_2 + (v \sin\theta_v)\ t, \tag{24}$$

$$g_3(t) = y_3 + (v \sin\theta_v)t, \tag{25}$$

$$g_4(t) = y_4 + (u \sin\theta_u)t, \tag{26}$$

The functions $h_1(t)$, $h_2(t)$, $h_3(t)$, $h_4(t)$, $g_1(t)$, $g_2(t)$, $g_3(t)$, $g_4(t)$, describe the movement along the *x* and *y* axis, respectively, and allow for the realization of a rectangular grid with stationary boundary conditions, *where* $h_0(t) = 0$, $h_5(t) = L_x$, $g_0(t) = 0$, $g_5(t) = L_y$, $0 \le \theta_u \le 360^o$, $0 \le \theta_v \le 360^o$. By choosing the angles, it is easy to apply this technique for the analysis of arbitrary motions. The partial time-derivatives in the transformed domain (ξ,η,τ) can be expressed in terms of the partial derivatives of the original domain *(x,y,t)* using eqs. (16)-(26). The FDTD technique can provide the time-domain solution of the rectangular (ξ,η,τ) grid. The stability criterion in this case is chosen as $c\ \Delta t \le \delta / 0.707$, where $\delta = \Delta x_o = \Delta y_o$ assuming the grid is uniformly discretized in both directions. In general, δ is the minimum space increment (minimum cell size) for *x* and *y* directions [8].

4. Numerical Results

To validate this approach, numerical results are calculated for a two-dimensional variable capacitor with its fingers moving only to the *x*-direction. The grid includes 200x200 cells where $L_x = L_y = L = 5\lambda$, $\Delta x = \Delta y = L/200$, and $\Delta t = L/800c$. In this case, as the plates are moving only to the *x*-direction away from each other, the angles are $\theta_u = 0^\circ, \theta_v = 180^\circ$ and as the plates are approaching other, the angles are $\theta_u = 180^\circ, \theta_v = 0^\circ$. The initial plate separation is $L/5$ and the grid is terminated with Mur's absorbing boundary conditions. The relation between the velocity and the transient value of the capacitance between the moving fingers, assuming that they start to move away and approach each other at t=40 time-step and stop at t=60 time-step, is shown in Fig. 2. The capacitance is derived from [15] and is calculated in the area of no.43 in Fig. 2. Theoretically, the value of the capacitance is derived from $C = \varepsilon_0 S/d$, where $d = \lambda$, $S = \lambda \times 1$. The stationary value (u=v=0) in Fig. 2, is agreed with this theoretical value. It can be observed that different velocity values lead to different values of the capacitance, since they

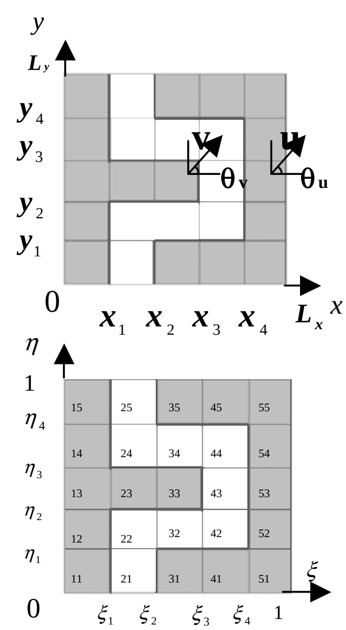

Fig. 1. Physical region (top graph) and computational (bottom graph) region.

affect the spacing of the fingers for a specific t_o time-step. Fig. 3 displays computational results of the time dependence of the transient capacitance for velocity values in the range of $u = v = 2\times10^{-3}c$ to $u = v = 8\times10^{-3}c$, assuming that the plates move away from each other from t=10 time-step to t=60 time-step. The horizontal axis indicates the normalized time expressed in time steps and the vertical axis indicates the value of the transient capacitance. The stationary value (v=u=0) is displayed for reference reasons and demonstrates a (smoother) time-variation due to the time evolution of the excitation function itself. In Fig. 4, the time dependence of the transient capacitance is demonstrated for various velocity values, assuming that the plates approach each other from t=20 time-step to t=60 time-step. Following this approach other, the angles are $\theta_u = 0^\circ, \theta_v = 180^\circ$ and as the plates are approaching other, the angles are $\theta_u = 180^\circ, \theta_v = 0^\circ$. The initial plate separation is $L/5$ and the grid is terminated with Mur's absorbing boundary conditions. The relation between the velocity and the transient value of the capacitance between the moving fingers, assuming that they start to move away and approach each other at t=40 time-step and stop at t=60 time-step, is shown in Fig. 2. The capacitance is derived from [15] and is calculated in the area of no.43 in Fig. 2. Theoretically, the value of the capacitance is derived from $C = \varepsilon_0 S/d$, where $d = \lambda, S = \lambda\times1$. The stationary value (u=v=0) in Fig. 2, is agreed with this theoretical value.

It can be observed that different velocity values lead to different values of the capacitance, since they affect the spacing of the fingers for a specific t_o time-step. Fig. 3 displays computational results of the time dependence of the transient capacitance for velocity values in the range of $u = v = 2\times10^{-3}c$ to $u = v = 8\times10^{-3}c$, assuming that the plates move away from each other from t=10 time-step to t=60 time-step.

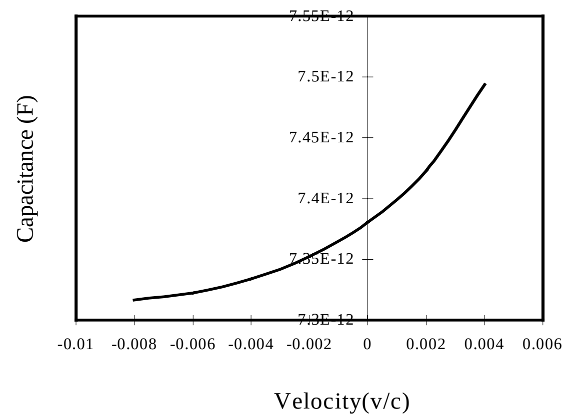

F ig. 2. Capacitance versus velocity.

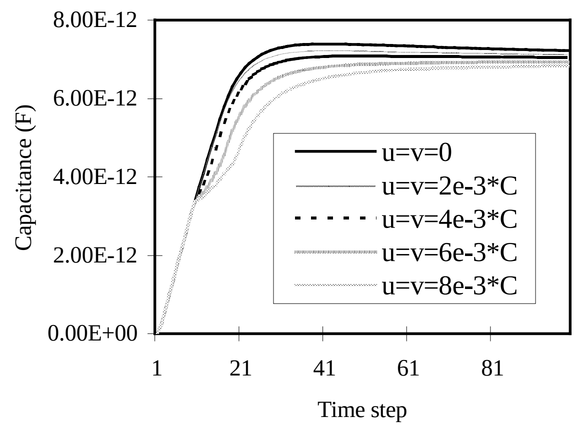

Fig. 3. Time dependence of transient capacitance for each velocity, where plates go away from t=10 time steps to t=60 time steps.

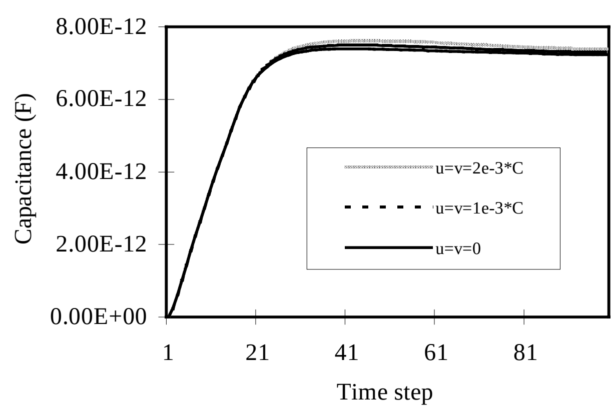

Fig. 4. Time dependence of transient capacitance for each velocity, where plates approach each other from t=10 time- steps to t=60 time-steps.

The horizontal axis indicates the normalized time expressed in time steps and the vertical axis indicates the value of the transient capacitance. The stationary value (v=u=0) is displayed for reference reasons and demonstrates a (smoother) time-variation due to the time evolution of the excitation function itself. In Fig. 4, the time dependence of the transient capacitance is demonstrated for various velocity values, assuming that the plates approach each other from t=20 time-step to t=60 time-step. Following this approach for the whole period of the motion of the fingers, it is easy to perform an accurate analysis of the transient response of the structure and predict the ringing parasitic effects. It is clear that the transient effect is more pronounced for the higher values of velocity.

Conclusions

A novel time-domain modeling technique that has the capability to accurately simulate the transient effect of variable capacitors with arbitrary in-plane motion of their plates has been proposed. This technique is a combination of the FDTD method and the body fitted grid generation technique. The key point of this approach is the enhancement of a space and a time transformation factor that leads to the development of a time-invariant numerical grid. The numerical results of the relation between the capacitance and the velocity of the motion are shown for a MEMS capacitor and demonstrate the proposed technique's unique computational advantages in the modeling of microwave devices with moving boundaries.

Acknowledgement

The authors wish to acknowledge the support of the Grant-in-Aid for Scientific Research ((c) No.13650435) of The Ministry of Education, Culture, Sports Science and Technology (MEXT), Japan and the NSF Career Award under #9984761, the Yamacraw Design Center of the State of Georgia and the Georgia Tech Packaging Research Center.

References

[1] A. Dec, K. Suyama, "Microwave MEMS-Based Voltage-Controlled Oscillators," *IEEE Trans. MTT*, pp. 1943-1949, vol.48, no. 11, Nov. 2000.

[2] N. Bushyager, B. McGarvey, M. Tentzeris, "Adaptive numerical modeling of RF Structures requiring the coupling of Maxwell's, mechanical and solid-state equations," *Proc. of the 2001 ACES*, pp. 1-6, Monterey, CA, March 2001.

[3] Mosher Rosenfeldm, Dochan Kwak, "Time dependent solution of viscous incompressible flow in moving co-ordinates", *International Journal. for Numerical Method in Fluid*, vol.13, pp. 1311-1328, 1991.

[4] S. Kuroda, H. Ohba, "Numerical analysis of flow around a rotation square cylinder," *JSME International Journal*, 36-4, B, pp. 592-597, 1993.

[5] C. Xu, M. Sen, M. Gad-el-Hak, "Dynamics of a Rotatable Cylinder with Splitter Plate in Uniform Flow," *Journal of Fluids and Structures*, Vol. 7, Issue 4, pp. 401-416, May 1993.

[6] P. J. Zwart, G. D.Raithby, "Space-time meshing for two dimensional moving boundary problems," *Proc. of the 7th International Meshing Roundtable*, Dearborn, Michigan, October 1998.

[7] M. Kuroda, "A dielectric waveguide with moving boundary," *IEICE Trans*., vol. E74, pp. 3952-3954, December 1991.

[8] M. Kuroda, "Electromagnetic wave scattering from perfectly conducting moving boundary-An application of the body fitted grid generation with moving boundary," *IEICE Trans.*, vol. E77-C, No.11, pp. 1735-1739, Nov. 1994.

[9] M. Kuroda, S. Kuroda, "FD-TD method for electromagnetic wave scattering from a moving body by using the body fitted grid generation with moving boundary", *Proc. of ICEAA99*, pp. 549-552, September 1999.

[10] M. Kuroda, S. Kuroda, "An application of body fitted grid generation method with moving boundaries to solve the electromagnetic field in a moving boundary," *Proc. of the*

2001 ACES, pp. 519-524, Monterey CA, March 2001.

[11] M. Kuroda, K Kawano, M. M. Tentzeris, “Body fitted grid generation method with moving boundaries and its application for analysis of MEMS devices,” *Proc. of the 2002 ACES*, pp. 219-224, Monterey CA, March 2002.

[12] M. Kuroda, N. Miura, M.M. Tentzeris, “A Novel Time-Domain Technique for the Analysis of MEMS-Based Variable Capacitors with Moving Metallic Parts,” *Proc. of APMC2002*, pp. III.1208-1211, Kyoto, JAPAN, November 2002.

[13] V. Bladel, “Relativity and Engineering,” *Springer-Verg*, Berlin, 1984.

[14] J. F. Thompson, “Numerical grid generation”, *North Holland*, Amsterdam, 1985.

[15] A. Taflove, S. Hagness, “Computational Electrodynamics, The finite difference time domain method,” Boston, Artech House, 2000.

Michiko Kuroda Professor Michiko Kuroda received the B. E. degree in Electrical Engineering from Shizuoka University, Shizuoka , Japan and the M. E. and D. E. in Electrical Engineering from Waseda University, Tokyo, Japan, She was a visiting researcher at the ElectroScience Laboratory, the Ohio State University, OH from 1986 to 1987. In 1990, she became an Associate Professor at Tokyo University of Technology. Since 1998, she has been a professor and in 2002 she became the Chair of the Department of Information Networks. She is a Correspondent of URSI (International Union of Radio Science) in Japan. Her research interests are FDTD method, grid generation method and its application for the moving boundary problems and MEMS devices.

Noriyuki Miura received the B. E. degree from Tokyo University of Technology, Tokyo, Japan in 2002. Now he is a graduate student at Tokyo University of Technology.

Manos M. Tentzeris Professor Manos M. Tentzeris received the Diploma Degree in Electrical and Computer Engineering from the National Technical University of Athens in Greece and the M.S. and Ph.D. degrees in Electrical Engineering and Computer Science from the University of Michigan, Ann Arbor, MI and he is currently an Assistant Professor with School of ECE, Georgia Tech, Atlanta, GA. He has published more than 100 papers in refereed Journals and Conference Proceedings and 4 book chapters. Dr. Tentzeris has helped develop academic programs in Highly Integrated Packaging for RF and Wireless Applications, Microwave MEM's, SOP-integrated antennas and Adaptive Numerical Electromagnetics (FDTD, Multi Resolution Algorithms) . He is the RF Alliance Leader of Georgia Tech NSF-Packaging Research Center and the leader of the Novel Integration Techniques Subthrust of the Broadband Hardware Access Thrust of the Yamacraw Research Initiative of the State of Georgia. He was the recipient of the 2003 IEEE CPMT Outstanding Young Engineer Award, the 2002 International Conference on Microwave and Millimeter-Wave Technology Best Paper Award (Beijing, CHINA) , the 2002 Georgia Tech-ECE Outstanding Junior Faculty Award , the 2001 ACES Conference Best Paper Award, the 2000 NSF CAREER Award and the 1997 Best Paper Award, International Hybrid Microelectronics and Packaging Society. He was also the 1999 Technical Program Co-Chair of the 54th ARFTG Conference, Atlanta, GA and he is the Vice-Chair of the RF Technical Committee (TC16) of the IEEE CPMT Society. Dr. Tentzeris was a Visiting Professor with the Technical University of Munich, Germany for the summer of 2002. He is a Senior Member of IEEE and a member of URSI and of the Technical Chamber of Greece.